



Biosorption of methylene blue dye by rice (*Oryza sativa* L.) straw: adsorption and mechanism study

Ali H. Jawad^{a,*}, Nurul Nadiah Mohd Firdaus Hum^a, Ahlam M. Farhan^b,
Mohd Sufri Mastuli^{a,c}

^aFaculty of Applied Sciences, Universiti Teknologi MARA, 40450 Shah Alam, Selangor, Malaysia, Tel. +60355211721; emails: ahjm72@gmail.com/ali288@uitm.edu.my (A.H. Jawad), Tel. +6035543 5737; email: nurulnadiyah@uitm.edu.my (N.N.M.F. Hum), Tel. +03 5543 6594; email: mohdsufri@uitm.edu.my (M.S. Mastulia)

^bChemistry Department, College of Sciences for Women, University of Baghdad, Baghdad, Iraq, Tel. (+964) 7702507225; email: ahlam63a@yahoo.com (A.M. Farhan)

^cCentre for Nanomaterials Research, Institute of Science, Universiti Teknologi MARA, 40450 Shah Alam, Selangor, Malaysia

Received 28 October 2018; Accepted 9 February 2020

ABSTRACT

In this work, rice (*Oryza sativa* L.) straw biosorbent (RSB) was evaluated as natural, renewable, and low-cost biosorbent for removal of methylene blue (MB) dye from aqueous solution. The structural characterization of the RSB was performed through pore structural analysis (Brunauer–Emmett–Teller), scanning electron microscopy and energy dispersive X-ray analysis, X-ray diffraction, Fourier transform infrared, point of zero charge method, and proximate analysis. Batch adsorption experiments were conducted to study the influence of adsorbent dosage (0.05–0.30 g), solution pH (2–12), initial dye concentration (20–100 mg/L), and contact time (0–240 min) on the adsorption of the MB. The kinetic uptake results were well described by the pseudo-second-order kinetic. The experimental data at equilibrium fitted well with the Langmuir model at 303°K, and the maximum adsorption capacity of MB on the RSB surface was found to be 158 mg/g. The mechanism of adsorption included mainly electrostatic attractions, n - π stacking interaction, and hydrogen bonding interaction. The results indicate the potential use of RBS as natural, renewable, and low-cost biosorbent for the removal of MB dye as a model of cationic dye.

Keywords: Adsorption; Agricultural waste; Rice straw; Low-cost adsorbent; Methylene blue

1. Introduction

Dyes are also known to be toxic and carcinogenic which could cause detrimental health effects. Nonetheless, the usages of synthetic dyes in various industries have increased significantly over the years due to its simple applicability and persistent dyeing effect [1]. Methylene blue (MB) dye, a cationic basic dye which forms face-to-face dimers, represents one of the most widely utilized synthetic dyes not only in the dyeing industries but also in the field of chemistry, biology, and medical science [2]. Some of the health

complications due to long term exposure to MB dye include eye burns, breathing difficulties, nausea, allergy, vomiting, mental confusion, jaundice, and even dysfunction of brain, liver, and central nervous system [3].

Various treatment methods are available for the removal of dyes from wastewater. These methods include biotreatment [4], flocculation–coagulation [5], photocatalytic degradation [6], Fenton chemical oxidation [7], cation exchange membranes [8], and electrochemical degradation [9]. Adsorption technique provides high performance and convenience of operation and selectivity as well as exhibits a simple design and flexibility [10]. Activated carbon is one of

* Corresponding author.

the most common adsorbent used for removal of dyes, nevertheless due to a high operational cost, and extremely difficult for regeneration limits its application on huge scale [11].

Taking these criteria into consideration, there is an interest to search for economic and efficient techniques using alternative materials such as agricultural waste as natural, renewable, and low-cost biosorbent. In recent years, adsorption process by biomass wastes has been regarded as the most affordable and feasible option for removal of dyes. Therefore, many types of agricultural residue and biomass waste were successfully utilized as renewable and low-cost biosorbent for removal of MB dye from aqueous such as pomegranate [12], dragon fruit peel [13], watermelon rinds [14], soft and hardwood wastes [15], rejected tea [16], tea waste [17], and canola residues [18].

Rice (*Oryza sativa* L.) is a prime source of carbohydrates in Asia. As per the Food and Agriculture Organisation of the United Nations (FAO) statistics in 2014, worldwide rice production was about 740 million tons [19]. So far, rice straw (RS) is considered as a waste, and consequently left or burnt without any profit. Numerous ideas have been suggested for exploiting RS as pulp and paper [20], construction materials [21], compost [22], fuel [23], production of ethanol [24], and precursor for activated carbon [25]. RS could be an excellent choice from an economic and environmental perspective due to its availability and zero value waste. To the best of our knowledge, RS so far never been applied as a biosorbent for removal of cationic dyes from wastewater. Therefore, this research work assesses the potential application of RS as a low-cost and renewable biosorbent for MB dye removal from aqueous solution through batch mode adsorption studies.

2. Materials and methods

2.1. Adsorbate (MB)

Methylene blue (MB, 98.5% Assay) as an adsorbate was bought from R&M Chemicals, Malaysia. All MB solutions were prepared and diluted with ultra-pure water. The used MB has a chemical formula of $C_{16}H_{18}Cl_3S \cdot xH_2O$ with molecular weight of 319.86 g/mol.

2.2. Preparation of adsorbent

The RS was collected from rice mill in Perlis, Malaysia. The dried RS was converted to very small pieces and washed several times with distilled water and then dried thoroughly in sunlight for 48 h. The dried RS was ground and sieved to the mesh size between 250 and 500 μm . Later, the RS was washed several times with distilled water, and then with ethanol technical grade to remove the dust and other water-soluble impurities and subsequently dried at 105°C for 24 h inside an oven. The obtained sample was converted into powder form by a mixer grinder and sieved to constant mesh size (250–500 μm). The final product of rice straw biosorbent (RSB) was stored in an airtight container for further applications.

2.3. Characterization of RSB

The physicochemical properties of RSB were investigated by using the following analyses. X-ray diffraction (XRD)

analysis was conducted in reflection mode (Cu $K\alpha$ radiation) on a PANalytical (UK), X'Pert Pro X-ray diffractometer. Scans were recorded with a scanning rate of 0.59°/s. The diffraction angle (2θ) was varied from 10° to 90°. Textural characterization of RSB was carried out by N_2 adsorption using Micromeritics ASAP 2060, USA. Fourier transform infrared (FTIR) spectral analysis of RSB was performed on a Perkin Elmer, Spectrum One in the 4,000–500 cm^{-1} wavenumber range. The surface physical morphology was examined by using scanning electron microscopy–energy-dispersive X-ray spectroscopy [(SEM–EDX (energy-dispersive X-ray), Hitachi, TM3030Plus, Tabletop Microscope, Japan)]. The pH at the point of zero charge (pH_{pzc}) was estimated using a pH meter (Metrohm, Model 827 pH Lab, Switzerland), as described by Lopez-Ramon et al. [26]. The surface charge (pHpzc) was measured by using the pH drift method with a pH meter, the solution pH was adjusted to a series of initial values between 2 and 12 by adding either HCl or NaOH and then RS (0.15 g) to the solution. These were then shaken for 24 h in an isothermal water bath shaker, a revolving water bath to reach equilibrium, after each resulting pH was measured and the initial pH (pH_0) vs. the difference between the initial and final pH values (ΔpH) was plotted. The pzc was taken as the point where $\Delta\text{pH} = 0$.

2.4. Batch adsorption experiments

The batch adsorption experiments were conducted in order to determine the optimized conditions of adsorbent dosage (0.05–0.30 g), solution pH (2–12), initial dye concentration (20–100 mg/L), and contact time (0–240 min). All experiments were performed in a series of conical flasks containing 100 mL of MB dye solution of known concentrations and the pH of MB solution was adjusted by adding either 0.10 mol/L HCl or 0.10 mol/L NaOH. A known dosage of RSB was added into the MB dye solution, capped, and agitated in a water bath shaker (Mettler, water bath, model WNB7–45, Germany) at a constant speed of 110 stroke/min and 303°K until equilibrium reached. The supernatant was separated using 0.20 μm Nylon syringe filter and the remaining dye concentration was monitored at different time intervals using a HACH DR 2800 direct reading spectrophotometer at a maximum wavelength (λ_{max}) of 661 nm. The blank test was carried out in order to account for color leached by the adsorbent and adsorbed by the glass containers, blank runs with the only RSB in 100 mL of doubly distilled water and 100 mL of MB solution without RSB were conducted simultaneously at similar conditions. The adsorption capacity at equilibrium, q_e (mg/g) and the percent of color removal, CR (%) of MB dye were calculated using Eqs. (1) and (2), respectively:

$$q_e = \frac{(C_0 - C_e)V}{W} \quad (1)$$

$$\text{CR}\% = \frac{(C_0 - C_e)}{C_0} \times 100 \quad (2)$$

where, C_0 (mg/L) = initial dye concentration; C_e (mg/L) = dye concentration at equilibrium; V (L) = volume of dye solution; W (g) = mass of adsorbent.

3. Results and discussion

3.1. Characterization of RSB

3.1.1. Physical properties of RSB

The results of physical and textural properties of RSB were recorded in Table 1. The results indicate that RSB has low values of bulk density, ash content, and moisture content, along with a relatively high yield approximate carbon. The N_2 adsorption/desorption isotherms for RSB is shown in Fig. 1, and the textural parameters of RSB are recorded in Table 1. As for textural properties, RSB has low Brunauer–Emmett–Teller (BET) surface area of 4.42 m^2/g . Pore sizes are classified in accordance with the IUPAC classification system (USA), where pores may possess variable diameter (d): micropores ($d < 2.0$ nm), mesopores (2.0 nm $< d < 50$ nm), and macropores ($d > 50$ nm) [27]. From the textural properties recorded in Table 1, it can be concluded that RSB is a mesoporous material.

3.1.2. Fourier transform infrared spectral analysis

FTIR spectral analysis elucidates the structural and compositional information on the active functional groups presented in the RSB. FTIR spectrum of RSB before adsorption (Fig. 2a) shows various functional groups, in agreement with their respective wavenumber (cm^{-1}) position. The broadband at 3,500 cm^{-1} is assigned to the overlapping of the stretching vibrations of the hydroxyl (O–H) and amine (N–H) groups, while band around 3,000 cm^{-1} is due to carboxylic acid O–H stretching. The band at 1,633 cm^{-1} associated with C=O (ketones, aldehydes, lactones, or carboxyl groups) [28]. The asymmetric and symmetric vibrations of $-COO$ of the ionic carboxylic groups within RSB are represented by the band at 1,523 cm^{-1} . The bands between the 1,300 and 1,000 cm^{-1} regions are assigned to the C–O and C–O–C stretching vibrations in carboxylic acids, alcohols, phenols, or ester groups [12–14]. Thus, the FTIR spectrum of RSB before adsorption indicates that the external surface of RSB is rich with various functional groups, containing oxygen of carboxylic and carbonyl species. These active groups on RSB surface are responsible for enhancing the adsorption of MB dye molecules due to electrostatic interaction. After MB dye adsorption (Fig. 2b), the band shifted and became more pronounced, and new bands assigned to nitro (1,274–1219 cm^{-1}) are attributed to MB dye loaded onto RSB surface.

Table 1
Physicochemical characterization of RSB

Properties/characteristics	Values
Bulk density (g/mL)	0.14
Ash content (wt.%)	9.44
Moisture content (wt.%)	3.15
Textural properties	
BET surface area (m^2/g)	4.42
Langmuir surface area (m^2/g)	6.69
Average pore width (nm)	29.8

3.1.3. Point of zero charge analysis

The pH_{zpc} analysis was studied to estimate the pH at which the net charge of the surface of adsorbent is zero. The pH_{zpc} of RSB was determined to find out the pH at which the electrical charge of the surface of RSB was zero. Fig. 3 shows that the pH_{zpc} of RSB was at pH 6.1 which reflected the acidity of RSB, this results in agreement with the aforementioned FTIR results (Fig. 2a) about the availability of acidic functional groups such as carboxylic acids, alcohols, phenols, or ester groups within the chemical structure of RSB. At solution pH above the pH_{zpc} value, the surface of RSB becomes negatively charged and thus, adsorption of cations is preferred [24]. In this regard, it is predicted that the adsorption of the cationic dye (MB dye) by RSB will be favorable at solution pHs above 6.1 due to electrostatic interactions.

3.1.4. X-ray diffraction spectral analysis

XRD analysis was performed to determine the degree of crystalline or amorphous nature of the RSB. Fig. 4 shows the XRD pattern of the RSB. The curve was indexed based on a standard diffraction reference pattern (PCPDF No: 898487). The X-ray diffractograms indicate the appearance of a broad diffraction background and the absence of a sharp peak reveals a predominantly amorphous structure. XRD peak at $2\theta = 24^\circ$ in the spectrum assigned to the reflection from (002) relates to crystalline carbon with expanded lattice parameters (carbon with impurities).

3.1.5. SEM–EDX analysis

The SEM and EDX results of RSB before and after MB dye adsorption are shown in Figs. 5a and b, respectively. As seen in Fig. 5a, the external surface of RSB displays a rough texture distributed over the surface. Additionally, the corresponding EDX spectrum (Fig. 5a) indicates that the RSB consists of mainly C and O, and a detectable amount of Si and N. After MB adsorption (Fig. 5b), the RSB surface is transformed to be more compact and smoother due to filling of MB dye molecules on the RSB surface. It was also observed from EDX results (Fig. 5b) that RSB consists of mainly C and O, and a detectable amount of Si and N. The slight increment in the

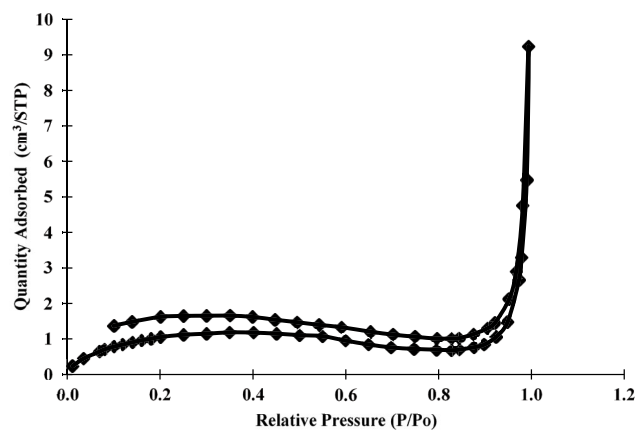


Fig. 1. Isotherms of N_2 adsorption–desorption for RSB.

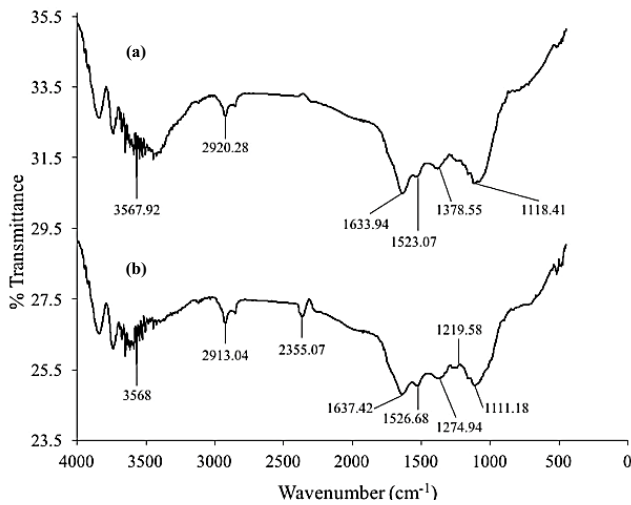


Fig. 2. FTIR spectra of (a) RSB, and (b) RSB after MB dye adsorption.

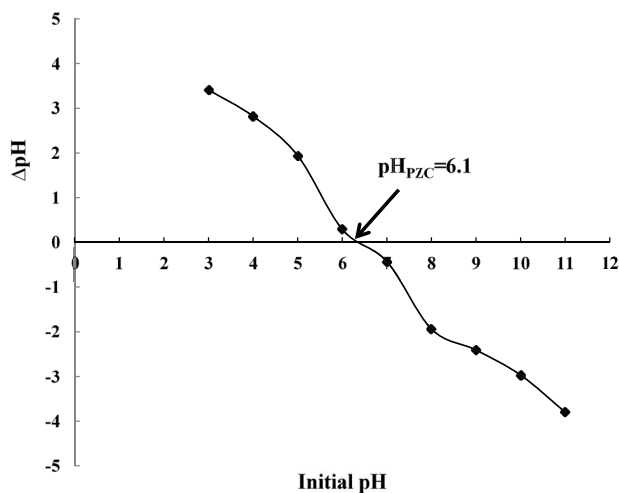


Fig. 3. pHpzc of RSB suspensions.

C, O, and N content of RSB after MB dye adsorption (Fig. 5b) can be attributed to the MB dye molecules loaded on the RSB surface.

3.2. Batch Adsorption Experiments

3.2.1. Effect of the adsorbent dosage

The influence of adsorbent dosage on the removal of MB dye from aqueous solution was studied using variable amounts of RSB ranging from 0.05 to 0.30 g at a fixed volume, 100 mL and initial dye solution, C_0 of 100 mg/L, while other experimental parameters were kept constant at 303°K, shaking speed of 110 stroke/min, a contact time of 60 min and non-adjusted pH at 6.1 for the MB solution. The result for adsorptive removal of MB dye with respect to adsorbent dosage is presented in Fig. 6. It is obvious that the removal of MB dye increases rapidly with an increase of RSB dosage due to the greater availability of the exchangeable active sites. The highest level of MB dye removal was achieved at

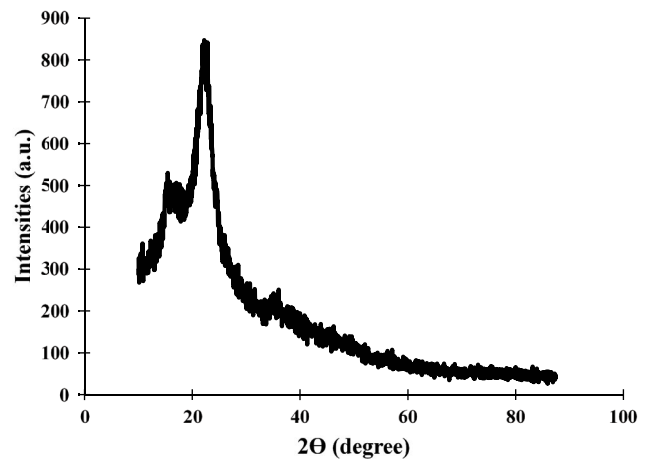


Fig. 4. XRD pattern of RSB.

RSB dose of 0.1 g/100 mL with 84.05% removal and thereafter, further increase of dosage did not exert an appreciable increase in the MB removal percentage. This situation can be explained by aggregate formation during adsorption, which takes place at high adsorbent concentrations causing a decrease in the effective adsorption areas [14]. Therefore, in further experiments the adsorbent dosage was fixed at 0.1 g for further investigations.

3.2.2. Effect of pH

The pH of solution was expected to influence the adsorption capacity of dyes as it has the ability to modify dyes chemistry and also the surface charge of the adsorbent. Fig. 7 shows the effect of pH on the adsorption of MB dye by RSB. The adsorption of MB dye by RSB increased steadily with the increasing solution pH up to pH 7.0. After that, a further increase in pH values demonstrated no obvious changes. At acidic pH, lower adsorption capacity were reported due to an additional concentration of H^+ ions competing with the MB dye cations for adsorption sites. At solution $pH < pH_{pzc} = 6.1$, the surface of RSB was essentially positively charged and thus, repulsion between the MB dye cations and the RSB may have occurred and decreased the MB dye adsorption capacity. On the other hand, At solution $pH > pH_{pzc} = 6.1$ as the solution pH of the system increased, the surface of RSB was likely to adopt negative surface charges and became increasingly favorable for MB adsorption due to electrostatic forces of attraction. In fact, at higher solution pH values, the surface of RSB adopts a negative surface charge, which contributes to enhanced uptake of positively charged dye species via attractive electrostatic attraction, in accordance with an increase in the rate of adsorption. To continue this work, the effective solution pH for RSB was fixed at 7, and used in further adsorption studies.

3.2.3. Effect of initial dye concentrations and contact time

The effect of concentrations and contact time is crucial for determining the time required for the adsorbent to achieved equilibrium. Fig. 8 displays the amounts of MB dye adsorbed (q_t) vs. time (min) at different initial MB dye

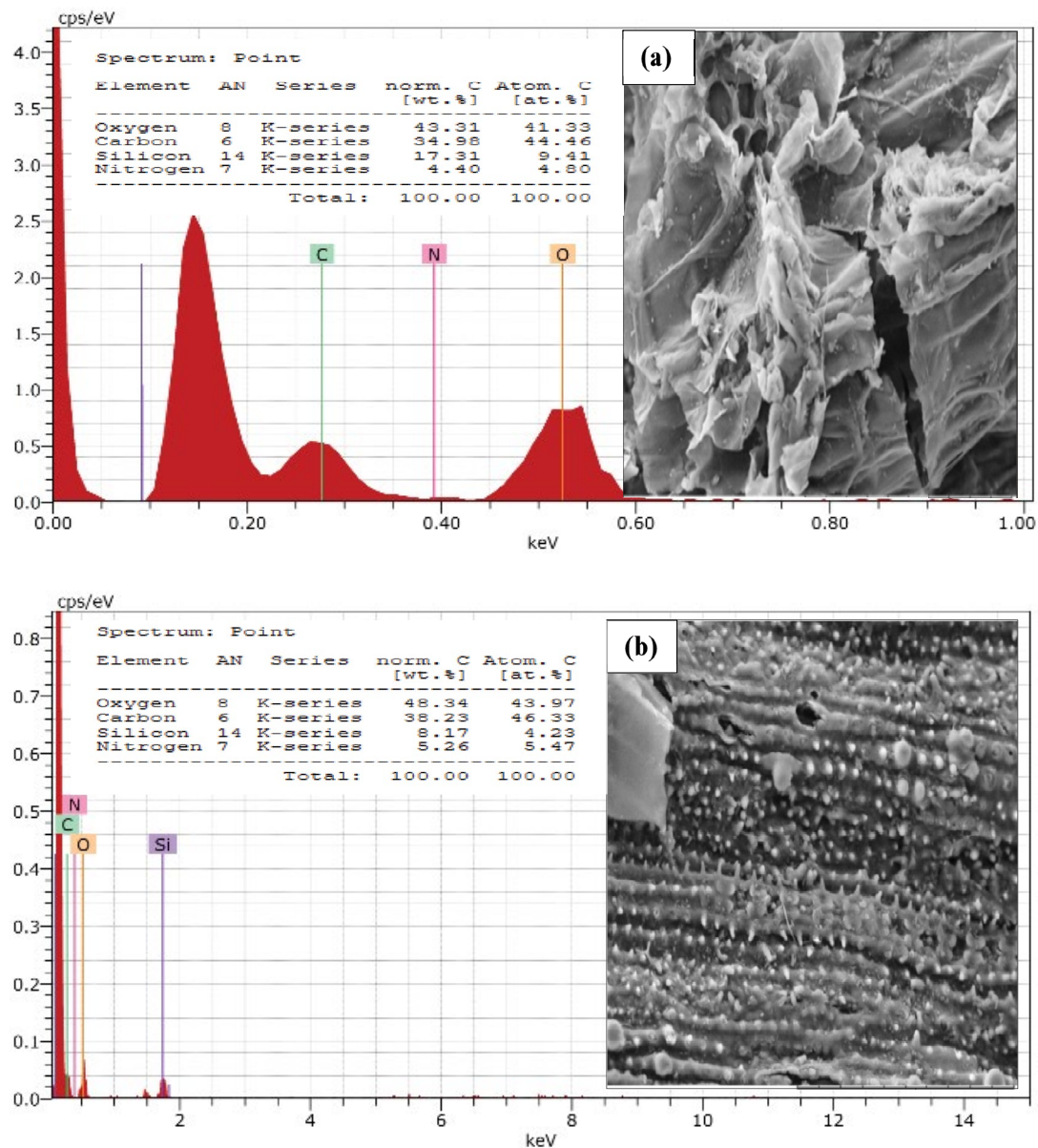


Fig. 5. SEM–EDX profiles for (a) RSB and (b) RSB after MB dye adsorption at magnification power (1,000 K).

concentrations. The time variation plot pointed out that the adsorption of MB dye was fast at initial stage. However, once equilibrium was nearly approached, the adsorption process slows down gradually. This situation may be due to the availability of unfilled active sites during the beginning stage of adsorption, and after a certain period of time, vacant sites get occupied by MB dye molecules, creating a repulsive force between MB dye, and RSB surface in the bulk phase. The amount of MB adsorbed by the RSB at equilibrium increases from 22.7 to 99.4 mg/g as the initial MB dye concentration increased from 20 to 100 mg/L. In batch adsorption experiments, the removal rate of the dyes from aqueous solutions is controlled by the transport of dye molecules from the surrounding sites to the interior sites of the adsorbent. High MB dye concentration not only provides a large driving force to

overcome all mass transfer resistances between the aqueous and solid phases, but also determines a higher probability of collision between MB dye ions and RSB surface. At higher MB dye concentrations, longer time was required for adsorption to complete, since there is a probability for MB dye molecules to penetrate deeper within the interior surface of the RSB and be adsorbed at active pore sites.

3.3. Adsorption isotherm

The adsorption isotherm is the most meaningful information which describes how the adsorbate molecules distribute between the solid-liquid phases when the adsorption process reaches an equilibrium state [29]. Three isotherm models, namely Langmuir [30], Freundlich [31], and Te

kin [32] were tested in this work. The Langmuir isotherm model Langmuir describes the monolayer adsorption process on uniform adsorption sites and is expressed by Eq. (3):

$$q_e = \frac{q_{max} K_a C_e}{1 + K_a C_e} \quad (3)$$

where, C_e (mg/L) = equilibrium adsorbate concentration; q_e (mg/g) = amount of adsorbed species per specified amount of adsorbent; k_L (L/mg) = Langmuir affinity constant; q_{max} (mg/g) = amount of adsorbate required to form an adsorbed monolayer.

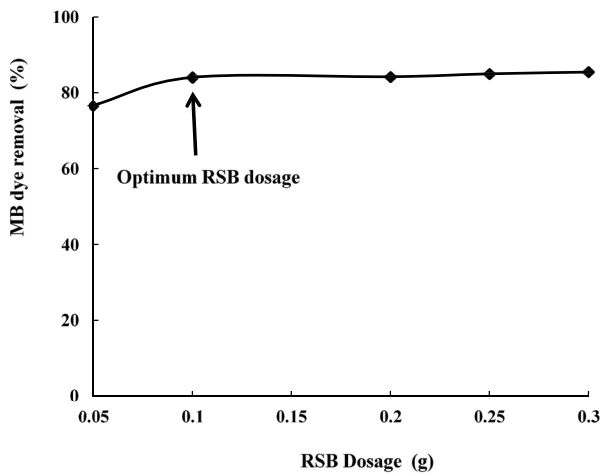


Fig. 6. Effect of RSB dosage on MB dye removal (%) at $[MB]_0 = 40$ mg/L, $V = 100$ mL, $pH = 5.6$, $T = 303$ K, shaking speed = 110 stroke/min, and contact time = 60 min.

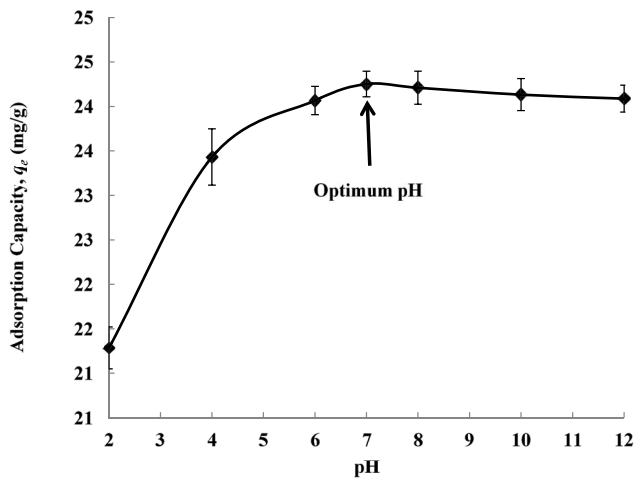


Fig. 7. Effect of pH on the adsorption capacity of MB dye by RSB at $[MB]_0 = 140$ mg/L, $V = 100$ mL, $T = 303$ K, shaking speed = 110 stroke/min, contact time = 60 min, and RSB dosage = 0.1 g.

Freundlich model is based on the assumption that multilayer adsorption process takes place on heterogeneous adsorption sites. Linear equation of Freundlich model is presented in Eq. (4):

$$q_e = K_F C_e^{1/n} \quad (4)$$

where, C_e (mg/L) = equilibrium adsorbate concentration; q_e (mg/g) = amount of adsorbate adsorbed per unit mass of adsorbent; $K_F [(mg/g (L/mg)^{1/n})]$ = Freundlich affinity constant.

Temkin model assumes that the heat of adsorption of all the molecules in the layer decreases linearly with coverage due to adsorbent/adsorbate interactions, and adsorption is characterized by a uniform distribution of binding energies, up to some maximum binding energy. Temkin isotherm can be expressed in its linear form is presented in Eq. (5):

$$q_e = \frac{RT}{b_T} \ln(K_T C_e) \quad (5)$$

where, C_e (mg/L) = equilibrium adsorbate concentration; q_e (mg/g) = amount of adsorbate adsorbed per unit mass of adsorbent; K_T (L/mg) = equilibrium binding constant; b_T = adsorption heat.

A non-linear plot of Langmuir, Freundlich, and Temkin models are shown in Fig. 9. The isotherm related parameters were calculated, and the results are shown in Table 2. Based on calculated data, Langmuir model shows best fit with the highest correlation coefficients, R^2 compared to Freundlich and Temkin models. The results show that the formations of a surface monolayer of MB dye molecules for RSB. Moreover, the monolayer adsorption capacity, q_m for RSB towards MB dye was compared with other types of biomass wastes as reported in Table 3. Therefore, the RSB utilized in this study can be considered as an effective biosorbent for removal of cationic dye like MB dye from aqueous solution.

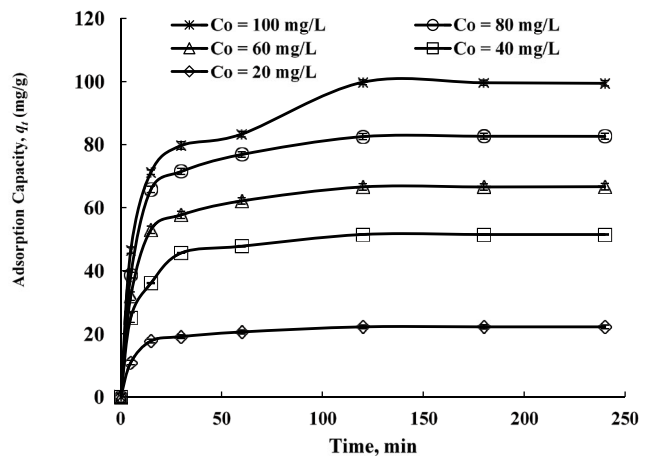


Fig. 8. Effect of initial concentration and contact time on the adsorption of MB dye by RSB at $V = 100$ mL, $T = 303$ K, $pH = 7$, shaking speed = 110 stroke/min, and RSB dosage = 0.1 g.

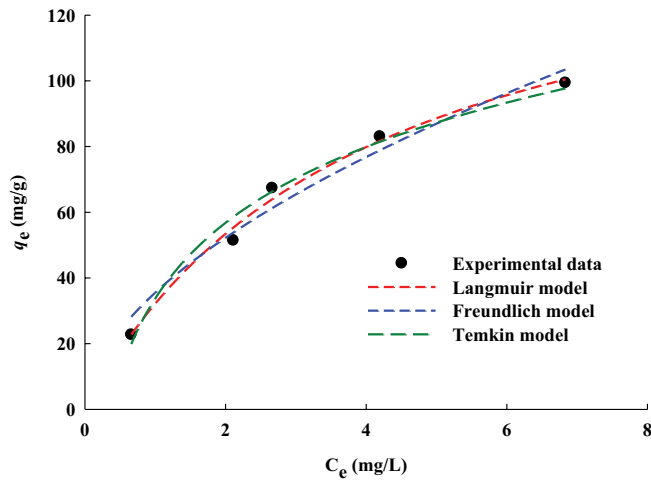


Fig. 9. Adsorption isotherm plots of the Langmuir, Freundlich, and Temkin models for MB dye adsorption by RSB at 303 K.

Table 2
Isotherm parameters for adsorption of MB dye by RSB at 303°K

Isotherm	Parameters	Values
Langmuir	q_{\max} (mg/g)	158
	K_L (L/mg)	0.25
	R^2	0.99
Freundlich	$K_f [(mg/g) (L/mg)^{1/n}]$	35.5
	$1/n$	0.55
	R^2	0.96
Temkin	b_T	77.4
	k_T (L/mg)	3.50
	R^2	0.98

3.4. Adsorption kinetic

Adsorption kinetic was studied in order to understand the controlling mechanism of adsorption process, such as mass transfer and chemical reactions. Two types of kinetic models namely pseudo-first-order (PFO) and pseudo-second-order (PSO) models were used to test the fit of experimental data of MB dye uptake by RSB. PFO was proposed by Lagergren [33] as given by Eq. (6):

$$q_t = q_e (1 - \exp^{-k_1 t}) \quad (6)$$

where, q_e (mg/g) = amount of adsorbate adsorbed per unit mass of adsorbent; q_t (mg/g) = amount of adsorbate adsorbed at any time; k_1 = PFO rate constant; q_e and k_1 values at different initial MB concentrations were calculated from the plots of $\ln(q_e - q_t)$ against t .

The linear form of the PSO model is given by Eq. (7) [34]:

$$q_t = \frac{q_e^2 k_2 t}{1 + q_e k_2 t} \quad (7)$$

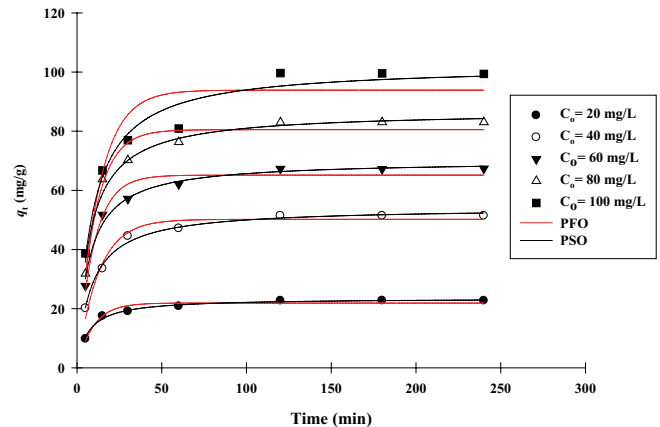


Fig. 10. Non-linear plots of the pseudo-first- and pseudo-second-order kinetic models for MB adsorption on RSB surface.

where, q_e (mg/g) = amount of adsorbate adsorbed per unit mass of adsorbent; q_t (mg/g) = amount of adsorbate adsorbed at any time; k_2 [mg/(min g)] = PSO rate constant.

The obtained results of these two kinetic models were shown in Fig. 10 and also reported in Table 4. As can be observed from the data, the value of correlation coefficient of the PSO kinetic model ($R^2 \geq 0.99$) was higher compared to the PFO kinetic model ($R^2 \leq 0.96$). Also, the quantity of theoretical q_e ($q_{e,cal}$) determined from the PSO was closer to the quantity of experimental q_e ($q_{e,exp}$). The results indicate that PSO has better fit than PFO for the process of MB dye adsorption by RSB. This result infers that the rate of MB dye adsorption onto RSB seems to be governed by chemical process that involved sharing of electrons or by covalent forces through exchanging of electrons between adsorbent and adsorbate. Similar finding was obtained for the adsorption of MB dye onto pomegranate peels [12], dragon fruit peels [13], and watermelon rinds [14].

3.5. Adsorption mechanism

The proposed adsorption mechanism of MB dye on the surface of RSB is presented in Fig. 11. Based on the various functional groups available on the surface of RSB as discussed previously in FTIR spectral analysis, the adsorption mechanism of MB dye can be attributed to the various interactions, for example, electrostatic attractions between negatively charged functional groups on the surface of RSB and positively charged species of the hydrolyzed cationic MB⁺ which strongly attracted from solution onto RSB surface [35], as sketched in Fig. 11a. Another important factor for MB dye adsorption by the RSB surface is the $n-\pi$ stacking interaction (Fig. 9b). In fact, the $n-\pi$ interaction generally occurs where the lone pair electrons on an oxygen atom are delocalized into the π orbital of an aromatic ring of dyes [36]. Another possibility of interaction is hydrogen bonding interaction between the surface hydrogen bonds of the functional groups available on the RSB surface and nitrogen atoms of the MB dye [35], as shown in Fig. 11c. Similar observations were reported by other researchers for the adsorption on MB dye on the surface of chemically treated carbon microspheres

Table 3
Adsorption capacities for MB dye by different biomass waste materials

Biomass waste	Adsorbent dosage (g)	pH	Temp. (K)	q_{\max} (mg/g)	References
Rice straw	0.1 g/100 mL	7.0	303	158	This Study
Softwood waste (Cedar)	0.8	6	298	217.3	[15]
Pomegranate peels	0.08/100 mL	5.6	303	200	[12]
Watermelon rinds	0.06 g/100 mL	5.6	303	188.6	[14]
Hardwood waste (Mahogany)	0.12	6	298	149.2	[15]
			303	147	
Rejected tea	0.25 g/100 mL	4.0	313	154	[16]
			323	156	
Tea waste	0.1 g/100 mL	8.0	303	85.1	[17]
Canola residues	0.35 g/100 mL	7.0	293	7.11	[18]

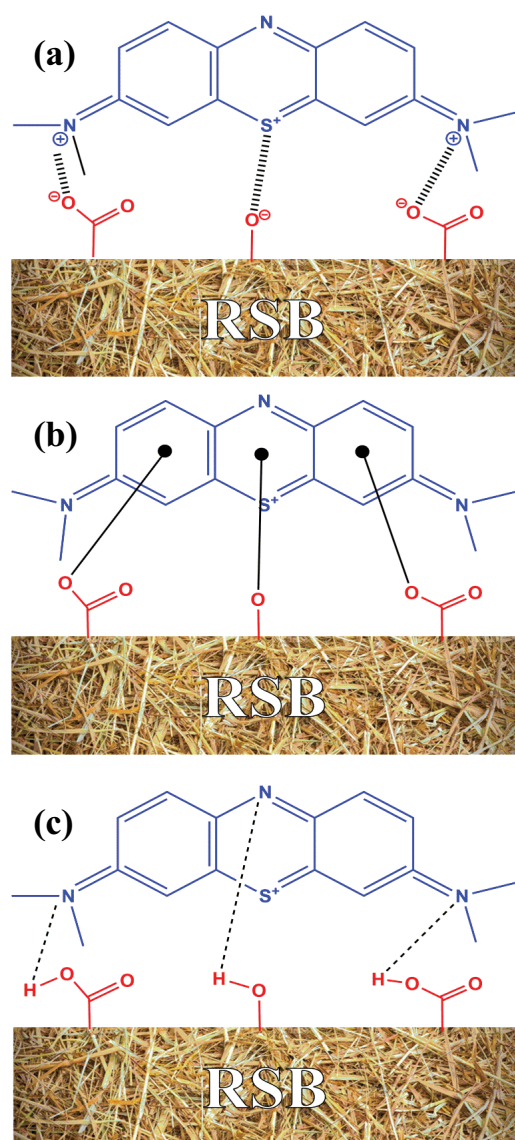


Fig. 11. Illustration of the possible interaction between RSB surface and MB dye: (a) electrostatic attraction, (b) $n-\pi$ stacking interactions, and (c) hydrogen bonding interactions.

Table 4
Parameters of the PFO and PSO kinetic models for MB adsorption by RSB at different initial MB dye concentration

Parameter	Concentration, C_0 (mg/L)				
	20	40	60	80	100
$q_{e,exp}$ (mg/g)	22.7	51.4	67.4	83.0	99.4
PFO					
$q_{e,cal}$ (mg/g)	46.1	65.9	88.5	103.1	142.2
$k_1 \times 10^{-2}$	3.16	3.58	3.57	5.31	1.93
R^2	0.94	0.96	0.95	0.96	0.87
PSO					
$q_{e,cal}$ (mg/g)	23.4	53.5	69.4	85.5	104.2
$k_2 \times 10^{-3}$	7.00	3.00	2.00	2.00	1.00
R^2	0.98	0.99	0.98	0.98	0.96

[37], multi-wall carbon nanotube [38], wrapping carbon nanotube [39], and coal activated carbon [35].

4. Conclusion

The research work clearly indicates that RSB provides a low-cost, renewable, and promising biosorbent for the removal of MB dye from aqueous solutions. The adsorption experiments indicated that the PSO model provided the best description of the kinetic uptake properties, while adsorption results at equilibrium are described by the Langmuir model where the maximum adsorption capacity, q_{\max} is 158 mg/g. The mechanism of MB dye adsorption on RSB included mainly electrostatic attractions, hydrogen bonding interaction, and $\pi-\pi$ stacking interaction. The results reveal that RSB a successful candidate for the removal of cationic dyes from aqueous solutions. The potential application of this material can be further extended toward removal of heavy metals, pesticides, and other colorless organic water pollutants.

Acknowledgments

The authors would like to thank the Universiti Teknologi MARA, Institute of Research Management, and Innovation

(Institut Pengurusan Penyelidikan and Inovasi) for supporting this project under LESTARI grant [600-IRMI 5/3/LESTARI (037/2019)].

References

- [1] M. Naushad, A.A. Alqadami, Z.A. AlOthman, I.H. Alsohaimi, M.S. Algamdi, A.M. Aldawsari, Adsorption kinetics, isotherm and reusability studies for the removal of cationic dye from aqueous medium using arginine modified activated carbon, *J. Mol. Liq.*, 293 (2019) 111442.
- [2] T. Tatarchuk, N. Paliychuk, R.B. Bitra, A. Shychuk, M. Naushad, I. Mironyuk, D. Ziolkowska, Adsorptive removal of toxic Methylene Blue and Acid Orange 7 dyes from aqueous medium using cobalt-zinc ferrite nanoadsorbents, *Desal. Water Treat.*, 150 (2019) 374–385.
- [3] M. Naushad, S. Vasudevan, G. Sharma, A. Kumar, Z.A. AlOthman, Adsorption kinetics, isotherms and thermodynamic studies for Hg²⁺ adsorption from aqueous medium using alizarin red-S loaded amberlite IRA-400 resin, *Desal. Water Treat.*, 57 (2016) 18551–18559.
- [4] A.R. Khataee, A. Movafeghi, S. Torbati, S.Y. Salehi Lisar, M. Zarei, Phytoremediation potential of duckweed (*Lemna minor* L.) in degradation of C.I. Acid Blue 92: artificial neural network modeling, *Ecotoxicol. Environ. Saf.*, 80 (2012) 291–298.
- [5] P. Canizares, F. Martnez, C. Jimenez, J. Lobato, M.A. Rodrigo, Coagulation and electrocoagulation of wastes polluted with dyes, *Environ. Sci. Technol.*, 40 (2006) 6418–6424.
- [6] A.H. Jawad, N.S.A. Mubarak, M.A.M. Ishak, K. Ismail, W.I. Nawawia, Kinetics of photocatalytic decolorization of cationic dye using porous TiO₂ film, *J. Taibah Univ. Sci.*, 10 (2016) 352–362.
- [7] Y.S. Woo, M. Rafatullah, A.F.M. Al-Karkhi, T.T. Tow, Removal of Terasil Red R dye by using Fenton oxidation: a statistical analysis, *Desal. Water Treat.*, 53 (2013) 1–9.
- [8] J.S. Wu, C.H. Liu, K.H. Chu, S.Y. Suen, Removal of cationic dye methyl violet 2B from water by cation exchange membranes, *J. Membr. Sci.*, 309 (2008) 239–245.
- [9] L. Fan, Y. Zhou, W. Yang, G. Chen, F. Yang, Electrochemical degradation of aqueous solution of Amaranth azo dye on ACF under potentiostatic model, *Dyes Pigm.*, 76 (2008) 440–446.
- [10] M. Rafatullah, O. Sulaiman, R. Hashim, A. Ahmad, Adsorption of methylene blue on low-cost adsorbents: a review, *J. Hazard. Mater.*, 177 (2010) 70–80.
- [11] R.A. Rashid, M.A.M. Ishak, K. Mohamed, Adsorptive removal of methylene blue by commercial coconut shell activated carbon, *Sci. Lett.*, 12 (2018) 77–101.
- [12] A.H. Jawad, A.S. Waheeb, R.A. Rashid, W.I. Nawawia, E. Yousif, Equilibrium isotherms, kinetics, and thermodynamics studies of methylene blue adsorption on pomegranate (*Punica granatum*) peels as a natural low-cost biosorbent, *Desal. Water Treat.*, 105 (2018) 322–331.
- [13] A.H. Jawad, A.M. Kadhum, Y.S. Ngoh, Applicability of dragon fruit (*Hylocereus polyrhizus*) peels as low-cost biosorbent for adsorption of methylene blue from aqueous solution: kinetics, equilibrium and thermodynamics studies, *Desal. Water Treat.*, 109 (2018) 231–240.
- [14] A.H. Jawad, Y.S. Ngoh, K.A. Radzun, Utilization of watermelon (*Citrullus lanatus*) rinds as a natural low-cost biosorbent for adsorption of methylene blue: kinetic, equilibrium and thermodynamic studies, *J. Taibah Univ. Sci.*, 4 (2018) 371–381.
- [15] M. El Hajam, N.I. Kandri, A. Harrach, A. Zerouale, Adsorption of Methylene Blue on industrial softwood waste “Cedar” and hardwood waste “Mahogany”: comparative study, *Mater. Today Proc.*, 13 (2019) 812–821.
- [16] N. Nasuha, B.H. Hameed, A.T.M. Din, Rejected tea as a potential low-cost adsorbent for the removal of Methylene Blue, *J. Hazard. Mater.*, 175 (2010) 126–132.
- [17] T. Uddin, A. Islam, S. Mahmud, Adsorptive removal of Methylene Blue by tea waste, *J. Hazard. Mater.*, 164 (2009) 53–60.
- [18] D. Balarak, J. Jaafari, G. Hassani, Y. Mahdavi, I. Tyagi, S. Agarwal, V.K. Gupta, The use of low – cost adsorbent (canola residues) for the adsorption of methylene blue from aqueous solution: isotherm, kinetic and thermodynamic studies, *Colloid Interface Sci.*, 7 (2015) 16–19.
- [19] Food and Agricultural Commodities Production, Food and Agriculture Organisation of the United Nations, 2017. Available at: <http://faostat.fao.org/site/339/default.aspx>.
- [20] Y. Fahmy, H. Ibrahim, Rice straw for paper making, *Cell. Chem. Technol.*, 4 (1970) 339–348.
- [21] H.S. Yang, D.J. Kim, H.J. Kim, Rice straw-wood particle composite for sound absorbing wooden construction materials, *Bioresour. Technol.*, 86 (2003) 117–121.
- [22] P. Songmuang, S. Luangsirorat, W. Seetanun, C. Kanareugsa, K. Imai, Long-term application of rice straw compost and yield of a Thai rice, RD-7, *Jpn. J. Crop Sci.*, 54 (1985) 248–252.
- [23] R.R. Bakker, B.M. Jenkins, R.B. Williams, Fluidized bed combustion of leached rice straw, *Energy Fuels*, 16 (2002) 356–365.
- [24] Y. Nakamura, T. Sawada, E. Inoue, Enhanced ethanol production from enzymatically treated steam-exploded rice straw using extractive fermentation, *J. Chem. Technol. Biotechnol.*, 76 (2001) 879–884.
- [25] M. Ahmedna, W.E. Marshall, R.M. Rao, Production of granular activated carbons from select agricultural by-products and evaluation of their physical, chemical and adsorption properties, *Bioresour. Technol.*, 71 (2000) 113–123.
- [26] M.V. Lopez-Ramon, F. Stoeckli, C. Moreno-Castilla, F. Carrasco-Marin, On the characterization of acidic and basic surface sites on carbons by various techniques, *Carbon*, 37 (1999) 1215–1221.
- [27] K.S.W. Sing, D.H. Everett, R.A.W. Haul, L. Moscou, R.A. Pierotti, J. Rouquérol, Reporting physisorption data for gas/solid systems with special reference to the determination of surface area and porosity, *Pure Appl. Chem.*, 57 (1985) 603–619.
- [28] D. Pathania, S. Sharma, P. Singh, Removal of methylene blue by adsorption onto activated carbon developed from *Ficus carica* bast, *Arab. J. Chem.*, 10 (2017) S1445–S1451.
- [29] N. Somsesta, V. Sricharoenchaikul, D. Aht-Ong, Adsorption removal of methylene blue onto activated carbon/cellulose biocomposite films: equilibrium and kinetic studies, *Mater. Chem. Phys.*, 240 (2020) 122221.
- [30] I. Langmuir, The adsorption of gases on plane surfaces of glass, mica and platinum, *J. Am. Chem. Soc.*, 40 (1918) 1361–1403.
- [31] H. Freundlich, Ueber die adsorption in Loesungen (Adsorption in solution), *Z. Phys. Chem.*, 57 (1906) 385–470.
- [32] M.J. Temkin, V. Pyzhev, Recent modifications to Langmuir isotherms, *Acta Phys. Chim.*, 12 (1940) 217–222.
- [33] S. Lagergren, Zur theorie der sogenannten adsorption geloster stoffe, *Kungl. Svenska Vetenskapsakad. Handl.*, 24 (1898) 1–39.
- [34] Y.S. Ho, G. McKay, Sorption of dye from aqueous solution by peat, *Chem. Eng. J.*, 70 (1998) 115–124.
- [35] A.H. Jawad, K. Ismail, M.A.M. Ishak, L.D. Wilson, Conversion of Malaysian low-rank coal to mesoporous activated carbon: structure characterization and adsorption properties, *Chin. J. Chem. Eng.*, 27 (2019) 1716–1727.
- [36] N.H. Yusof, K.Y. Foo, B.H. Hameed, M.H. Hussin, H.K. Lee, S. Sabar, One-step synthesis of chitosan-polyethyleneimine with calcium chloride as effective adsorbent for Acid Red 88 removal, *Int. J. Biol. Macromol.*, (2018). doi: 10.1016/j.ijbiomac.2019.11.218.
- [37] Z. Jia, Z. Li, S. Li, Y. Li, R. Zhu, Adsorption performance and mechanism of methylene blue on chemically activated carbon spheres derived from hydrothermally-prepared poly(vinyl alcohol) microspheres, *J. Mol. Liq.*, 220 (2016) 56–62.
- [38] L. Aia, C. Zhang, F. Liao, Y. Wang, M. Li, L. Meng, J. Jiang, Removal of methylene blue from aqueous solution with magnetite loaded multi-wall carbon nanotube: kinetic, isotherm and mechanism analysis, *J. Hazard. Mater.*, 198 (2011) 282–290.
- [39] Z. Zhang, X. Xu, Wrapping carbon nanotubes with poly (sodium 4-styrenesulfonate) for enhanced adsorption of methylene blue and its mechanism, *Chem. Eng. J.*, 256 (2014) 85–92.